Evaporation of the ammonia from the solution described above leaves the solid potassium salts of the two anion radicals and the neutral nitrobenzenes in the reaction apparatus. The neutral nitrobenzenes can be easily distilled from this mixture under high vacuum, leaving only the solid K^+PhNO_2-$^{14}N^{-\cdot}$ and K^+PhNO_2-$^{15}N^{-\cdot}$. Recovery of the isotopically mixed nitrobenzenes is easily accomplished by reacting the solid anion radical salts with iodine dissolved in diethylether. The extra electrons are transferred from the anion radical to the I_2 to form I^- as shown in reaction (2):

[redacted]

Received 25 March; accepted 14 July 1986.

1. Tanaka, N., Yamaguchi, A. & Arki, M. *J. Am. chem. Soc.* 107, 7781–7782 (1985).
2. Stevenson, G. R., Espe, M. P. & Reiter, R. C. *J. Am. chem. Soc.* 108, 532–533 (1986).
3. Stevenson, G. R. & Hashim, R. T. *J. Am. chem. Soc.* 107, 5794–5795 (1985).
4. Lawler, R. D. & Fraenkel, G. K. *J. chem. Phys.* 49, 1126–1139 (1969).
5. Lawler, R. G. & Tabit, C. T. *J. Am. chem. Soc.* 91, 5671–5672 (1969).
6. Khatkale, M. S. & Devlin, J. P. *J. chem. Phys.* 70, 1851–1859 (1979).

Evaporative cooling of the

[redacted]

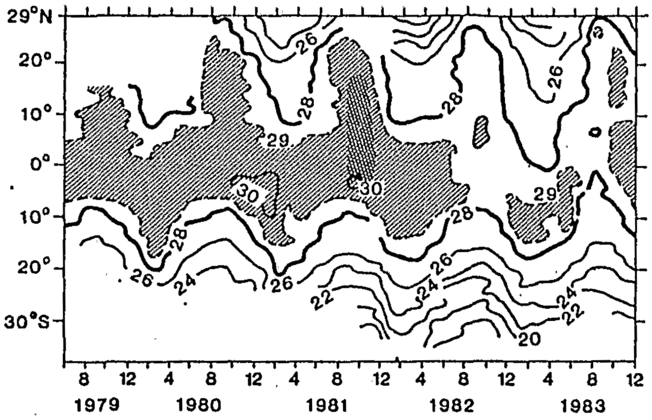

Fig. 1 Sea surface temperature on the shipping route between New Caledonia (or New Zealand) and Japan. Temperatures exceeding 29 °C are highlighted with single hatching. Double hatching indicates questionable values due to sparse data.

The processes that influence mixed-layer temperature are surface fluxes, horizontal advection by currents, entrainment mixing, turbulent diffusion, and penetrative radiation at D_{26} (refs 11, 12). The last two of these were found to be small in the equatorial Indian Ocean[11], and zonal advection is negligible. In the first model to be tested, the total surface flux (Q_T) is related to the change in upper-layer temperature by the relation

$$\rho C D_{26} \frac{\partial T_{26}}{\partial t} = Q_T \qquad (1)$$

where ρ and C are the density and heat capacity of water, and t is time. It is assumed in equation (1) that the mean surface flux is independently balanced by diffusion and advection, thus the equation applies only to fluctuations.

The local rate of heat storage, the left-hand side of equation (1), was calculated from T_{26} and D_{26}, and is typically of the order ± 40 W m^{-2} (Fig. 2*f*). Periods of persistent cooling seen in T_{26} (Fig. 2*a*) are associated with the largest negative values of heat storage, as indicated by horizontal brackets. We seek an explanation for these cooling events.

The surface heat fluxes (insolation and net long-wave radi-

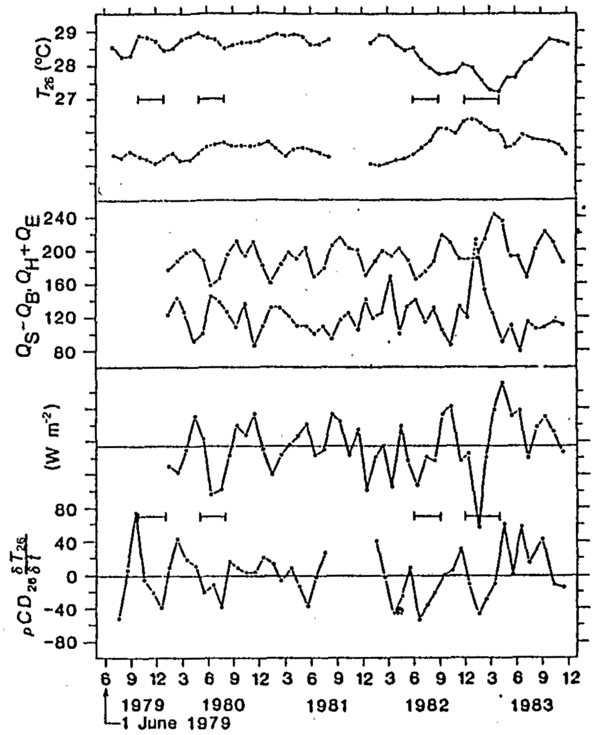

Fig. 2 *a*, Upper-layer temperature (T_{26}) averaged between the surface and the depth of the 26 °C isotherm (*b*, D_{26}). Heat fluxes at the sea surface: *c*, net radiation (Q_S-Q_B); *d*, net latent and sensible heat flux (Q_E+Q_H); *e*, total heat flux (Q_T), obtained by subtracting curve *d* from curve *c*; *f*, local heat storage rate ($\rho C D_{26}\, \partial T_{26}/\partial t$). Horizontal bars bracket times of largest cooling events.

the mean value (75 W m^{-2}) for the 1979–83 period. The correlation coefficient is 0.45, which is significant at the 5% level, allowing for a decorrelation timescale of 2 months.

The next question is, which fluxes have the greatest effect on heat storage rates? Visual inspection of Fig. 2 suggests that changes are due more to irregular fluctuations in turbulent flux than to semi-annual oscillations in radiative flux. The correlations of the heat storage rate [$\rho c D_{26}(\partial T_{26}/\partial t)$] with each of the

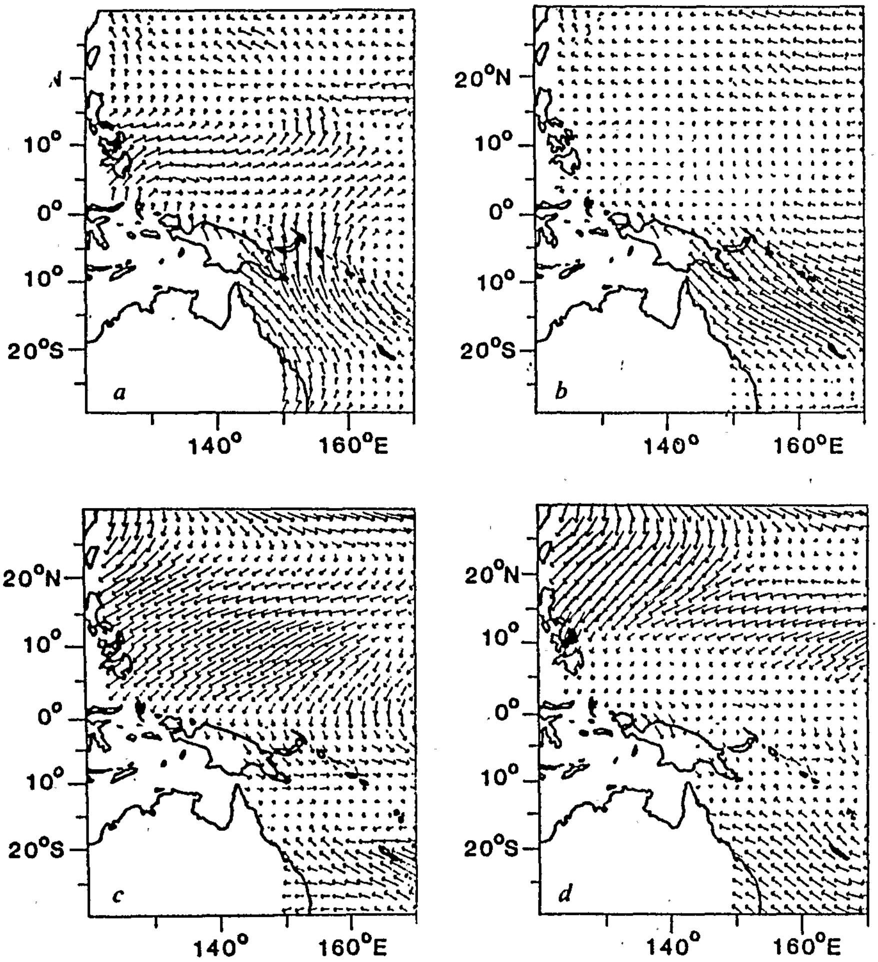

Fig. 3 The field of wind stress at the sea surface during two anomalous cooling periods in 1982–83 (*a*, July 1982; *c*, January 1983) and during two normal periods in 1981 (*b*, July 1981; *d*, January 1981).

where primes indicate that each parameter is measured relative to its mean value and normalized by its standard deviation.

variable wind field is seen near the Equator (Fig. 3*d*). Cooling meridional wind coming from the winter hemisphere is probably

John Horel suggested a study of the role of western Pacific temperature in the Southern Oscillation. This research was supported by NSF grants during the Pacific Equatorial Ocean Dynamics (PEQUOD) programme, and by the Equatorial Pacific Ocean Climate Studies (EPOCS) programme of NOAA, and is contribution number 824 from the Pacific Marine Environmental Laboratory.

Received 6 May; accepted 17 July 1986.

1. Gill, A. E. & Rasmusson, E. M. *Nature* **306**, 229-234 (1983).
2. Cane, M. G. *Science* **222**, 1189-1194 (1983).
3. Nicholls, N. *Nature* **307**, 576-577 (1983).
4. Wyrtki, K. *J. geophys. Res.* **90**, 7129-7132 (1985).
5. Busalacchi, A. J., Takeuchi, K. & O'Brien, J. J. *J. geophys. Res.* **88**, 7551-7562 (1983).
6. Harrison, D. E. & Schopf, P. S. *Mon. Weath. Rev.* **112**, 923-933 (1984).
7. Palmer, T. N. & Mansfield, D. A. *Nature* **310**, 483-485 (1985).
8. Simmons, A. J. *Q. J. R. met. Soc.* **108**, 503-534 (1982).
9. Harrison, D. E. *Science* **224**, 1099-1102 (1984).
10. Meyers, G. & Donguy, J. R. *Nature* **312**, 258-260 (1984).
11. McPhaden, M. J. *J. mar. Res.* **40**, 403-419 (1982).
12. Stevenson, J. W. & Niiler, P. P. *J. phys. Oceanogr.* **13**, 1894-1907 (1983).
13. Reed, R. K. *J. geophys. Res.* **88**, 9627-9638 (1983).
14. Meyers, G. *J. phys. Oceanogr.* **12**, 1161-1168 (1982).
15. Lorenz, E. N. *Empirical Orthogonal Functions and Statistical Weather Prediction* (Science Rep. No. 1, Statistical Forcasting Project, MIT Department of Meteorology, Cambridge, 1956).
16. Legler, D. M. & O'Brien, J. J. *Atlas of Tropical Pacific Wind-Stress Climatology 1971-80* (Department of Meteorology, Florida State University, Tallahassee, 1984).
17. Leetma, A. & Wittee, J. (eds) *El Niño Atlas 1982-83* (Nova University Oceanographic Center Dania, 7L 33004, 1984).
18. Arkin, P. A., Kopman, J. D. & Reynolds, R. W. *1982-1983 El Niño/Southern Oscillation Event Quick Look Atlas* (NOAA National Weather Service, Washington DC, 1983).
19. Hasselmann, K. *Tellus* **28**, 473-485 (1976).
20. Nicholls, H. *Mon. Weath. Rev.* **112**, 424-432 (1984).
21. Philander, S. G. H. & Seigel, A. D. *Proc. 16th int. Liege Colloq. on Ocean Hydrodynamics* (ed. Nihoul, J.) (Elsevier, Amsterdam, 1985).

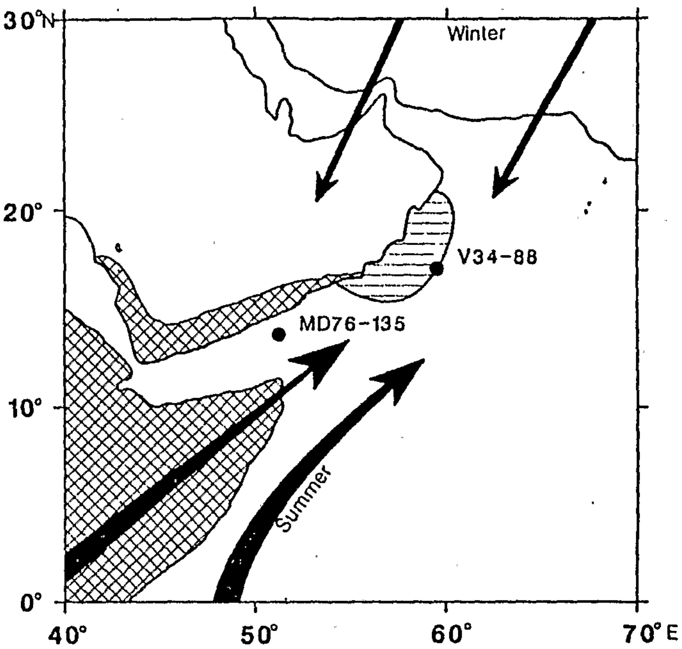

Fig. 1 Location of cores MD76-135 (containing the monsoon pollen index, MPI) and V34-88 (containing the monsoon upwelling index, MUI). The generalized source area for the MPI[26,27] is indicated by the cross-hatched pattern, and the area of maximum upwelling and MUI[11,12,23-25] is shown by horizontal shading. Arrows indicate the direction and relative strength of summer southwesterly and winter northeasterly winds.

Coherent response of Arabian Sea upwelling and pollen transport to late Quaternary monsoonal winds

Warren L. Prell* & Elise Van Campo†

* Department of Geological Sciences, Brown University, Providence, Rhode Island 02912, USA
† Laboratoire de Palynologie, Université de Sciences et Techniques du Languedoc, 34060 Montpellier Cedex, France

The Indian summer monsoon causes large seasonal changes in the environments of both eastern Africa and the Arabian Sea. Here we compare time series (140 kyr long) of selected pollen types and foraminiferal upwelling faunas preserved in marine sediments, to identify the frequencies of their variability and the coherence and phase of the terrestrial and marine responses to monsoonal circulation. During interglacial intervals, the pollen and upwelling records of the western Arabian Sea indicate stronger monsoons and are both coherent and in phase at periodicities near the precession of the Earth's rotational axis (23 kyr). We conclude that the strength

winds (Fig. 1), coastal upwelling (Fig. 1), and increased precipitation[1-5]. Changes in these climatic variables have been inferred from a large variety of geological data, including palaeolake levels[6,7], pollen spectra[8,9], wind-transported materials[10], and distribution of planktonic faunas[11-13]. These studies indicate that the monsoon was weaker ~18,000 yr ago, during maximum glacial conditions[14-17], and stronger ~9,000 yr ago, when the Northern Hemisphere received ~7% more summer insolation than at present[4-7,11,17,18]. Although the monsoonal circulation affects both continents and oceans, relatively few studies have compared the responses of these two environments. However, some studies have been able to document the abundance of terrestrial components, such as pollen[8,9,17], fresh-water diatoms[10] and phytoliths[10] in marine sediments, and thereby take advantage of the continuous and well-dated nature of marine records. In the western Arabian Sea, records of monsoonal upwelling faunas and wind-transported pollen are preserved in the deep-sea sediments. Our objective here is to determine the coherence of these marine and terrestrial data